Computer Assisted Mechanics and Engineering Sciences, 9: 191–203, 2002.

Structural optimization method based on cellular automata simulation *

Tetsuya Toyoda
Department of Mechano-Informatics and Sciences, Nagoya University, Nagoya, 464-8603 Japan

Eisuke Kita
School of Informatics and Sciences, Nagoya University, Nagoya, 464-8601 Japan

(Received May 29, 2000)

This paper describes the topology and the shape optimization scheme of the continuum structures using the cellular automata simulation. The design domain is divided into small square cells. By considering the cells as the elements, the stress analysis of the structure is carried out by finite element method. Then, the design variables are updated according to the local rule and the stress distribution. The rule is defined as the simple relationship between a cell whose design variable is updated and its neighborhood cells. In this paper, we will discuss the formulation to analytically derive the rules from the optimization problems. The special constraint condition named as "CA-constraint condition" is introduced first and then, the global optimization problem for the whole structure is divided into the local problem for some neighboring cells. The derived rules are applied to the same numerical example in order to discuss the theoretical validity of the formulation and the feature of the rules.

Keywords: topology and shape optimization, cellular automata (CA), local rule, 2D elastic problem, finite element method (FEM)

1. Introduction

John von Neumann first presented the theory of the finite automaton in 1950 and then, according to Ulam's suggestion, remade it to what we now call the cellular automaton [15, 22]. His studies are summarized as the theory of self-reproducing automata by Burks [16, 17]. Conway developed the Game of Life, which is one of the most famous application of the cellular automata [2]. Besides, Wolfram proved that the result of the liquid flow simulation by the cellular automata theoretically agrees with that obtained from the Navie-Stokes equations [23]. Since then, the cellular automata simulation is applied widely to several problems such as computer graphics, traffic flow simulation, structural optimization and so on [3, 4].

Structural optimization methods using the cellular automata have been studied by Xie et al. [9, 24–30], Inou et al. [5–7], Oda et al. [13, 14, 21], Ishida et al. [8], Kita et al. [10–12] and Payton et al. [18–20]. In Evolutionary Structural Optimization (ESO) method presented by Xie et al. [24], the design domain occupied by the structure is divided into small square cells. Considering the cells as the elements, the stress analysis of the structure is performed by the finite element method. When the magnitude of the state function at an element is larger than the reference value specified in advance, the cell is deleted. They firstly applied it to the elasto-static problem of the structure and then, extended to the other problems [24–27, 29, 30]. Besides, they also presented the Bi-directional Evolutionary Structural Optimization (BESO) Method [28] which not only delete cells but also can add new cells and the reduction scheme of the computational cost of the ESO method [9]. Evolutionary Structural Optimization method is considered as one of the primary studies in the structural optimization methods using cellular automata. Inou et al. [5–7] firstly introduced the concept of the cellular automata to the structural optimization. In their scheme, the reference stress at each cell is updated according to the local rule and then, the Young's modulus at the cell is modified so as to minimize the difference between the reference stress and the equivalent stress at the cell. The local rule is defined as the non-linear relationship between the equivalent stress and the Young's modulus from some numerical experiments. The ways to derive the local rule have been studied by Oda et al. [14], Payton et al. [18–20] and Kita et al. [10–12]. Oda et al. [14] presented the Evolutionary Cellular Automaton method, in which the local rule is defined by using the artificial neural network and evolved by the back propagation scheme. Payton et al. [18–20] derived the local rule from the local remodeling function of a bone adaptation algorithm. On the other hand, the authors presented the analytical derivation of the local rule from the optimization problem [10–12]. In these papers, minimizing the total weight of the structure and obtaining mean stress distribution on the structure were considered as the objective functions. The special constraint condition was introduced for deriving the local rule. The penalty function was defined from the objective functions and the constraint conditions and then, the local rule is derived from stationalizing it. The derived rule was applied to the simple numerical example. The final profile satisfying the design objects could be obtained but the convergence speed was fairly slow. This paper describes different formulation for improving the convergence speed.

This paper is organized as follows. In Section 2, the finite element formulation for the two-dimensional elastic problems is described briefly. In Section 3, three rules are derived and in Section 4, the rules are applied to the numerical example in order to compare their properties. Section 5 describes the way to improve the rule still more. Finally, Sections 6 and 7 describe some conclusions.

2. FINITE ELEMENT METHOD

2.1. Basic relationships

When the external forces are not applied to the body, the principle of the virtual work in the two-dimensional elastic problem is given as [1, 31]

$$\int_{\Omega} \delta \boldsymbol{\varepsilon}^T \boldsymbol{\sigma} \, d\Omega = \int_{\Gamma_t} \delta \mathbf{u}^T \bar{\mathbf{t}} \, d\Gamma, \tag{1}$$

where Ω, Γ_u and Γ_t ($\Gamma = \Gamma_u \bigcap \Gamma_t$) denote the domain occupied with the object under consideration, its displacement- and the traction-specified boundaries, respectively. Besides, $\mathbf{u}$, $\mathbf{t}$, $\boldsymbol{\varepsilon}$ and $\boldsymbol{\sigma}$ denote the displacement, the traction, the strain and the stress components in the two-dimensional elastic problem, respectively. The notation δ and the superscript T mean the virtual quantities and the transverse of the matrices and the vectors, respectively. The following relationships are hold among the physical quantities,

$$\begin{aligned} &\text{Displacement-strain relationship:} && \boldsymbol{\varepsilon} = \mathbf{A}\mathbf{u}, \\ &\text{Stress-strain relationship:} && \boldsymbol{\sigma} = \mathbf{D}\boldsymbol{\varepsilon}, \\ &\text{Cauchy relationship:} && t_i = \sigma_{ij} n_j, \end{aligned} \tag{2}$$

where $\mathbf{A}$ and $\mathbf{D}$ denote the matrix related to the partial differential operators and the stiffness matrix, respectively. n_j means the x_j-directional component of the unit normal vector on the boundary.

2.2. Discretization

Discretizing with N_e finite elements and approximating the displacement components of each element with the interpolation function $\mathbf{N}$ with nodal values $\mathbf{U}_e$, the left hand side of Eq. (1) leads to

$$\mathbf{u}_e = \mathbf{N}\mathbf{U}_e . \tag{3}$$

The strain and the stress components are given as

$$\boldsymbol{\varepsilon}_e = \mathbf{A}\mathbf{u}_e = \mathbf{A}\mathbf{N}\mathbf{U}_e \equiv \mathbf{B}\mathbf{U}_e , \tag{4}$$

$$\boldsymbol{\sigma}_e = \mathbf{D}\boldsymbol{\varepsilon} = \mathbf{D}\mathbf{B}\mathbf{U}_e . \tag{5}$$

The above equations are substituted into the left hand side of Eq. (1),

$$\sum_{e=1}^{N_e} \int_{\Omega_e} \delta\boldsymbol{\varepsilon}_e^T \boldsymbol{\sigma}_e \, d\Omega = \sum_{e=1}^{N_e} \int_{\Omega_e} (\mathbf{B}\delta\mathbf{U}_e)^T \mathbf{D}\mathbf{B}\mathbf{U}_e \, d\Omega \equiv \sum_{e=1}^{N_e} \delta\mathbf{U}_e^T h_e \mathbf{K}_e' \mathbf{U}_e , \tag{6}$$

where h_e and $\mathbf{K}_e'$ denote the thickness of the element and the elemental stiffness matrix, respectively. The subscript e denotes the number of the element.

Discretizing the right hand side of Eq. (1) with N_l boundary elements, we have

$$\int_{\Gamma_t} \delta\mathbf{u}^T \bar{\mathbf{t}} \, d\Gamma = \sum_{i=1}^{N_l} \int_{\Gamma_t} (\mathbf{N}\delta\mathbf{U})^T \bar{\mathbf{t}} \, d\Gamma \equiv \sum_{l=1}^{N_l} \delta\mathbf{U}_l^T \mathbf{f}_l' , \tag{7}$$

where $\mathbf{f}_l'$ and l denote the equivalent nodal force vector and the number of the boundary element, respectively.

Substituting Eqs. (6) and (7) to Eq. (1) leads to

$$\mathbf{K}\mathbf{U} = \mathbf{f} \tag{8}$$

which is solved for the displacement vector $\mathbf{U}$ by applying the boundary conditions.

3. LOCAL RULE

In this section, we shall describe how to derive the local rules from the optimization problems of the structures.

3.1. CA-formulation of structures

The design domain is divided into small square cells for the cellular automata simulation. The thicknesses of the cells are taken as the design variables and therefore, the cell thickness acts as the state quantity of the cell in the cellular automata simulation.

The quantity is updated at each time step according to the local rule and the state quantities of cells. The relationship between a cell whose quantity is updated and its neighboring cells is defined as the so-called Moor neighborhood (Fig. 1). In this figure, the center cell is named as "the updated cell" whose quantity is updated in this neighborhood relationship according to the local rule. The other cells are named as "neighborhood cells" for the updated cell. The updated cell is referred to as the cell 0 and the neighborhood cells are as the cell 1 to the cell 8.

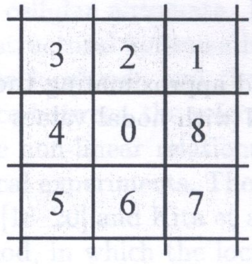

Fig. 1. Moor neighborhood

3.2. Rule 1

The design objectives are to minimize the total weight of the structure and to obtain the mean distribution of the Mises equivalent stress on the whole structure. The thickness of the updated cell is taken as the design variable. The CA-constraint condition is introduced in order that the global optimization problem for the whole structure is divided into the local optimization problem for each cell. The CA-constraint condition is defined so that the variation of the Mises equivalent stresses at the neighborhood cells with respect to the design variable is very small or equal to zero.

3.2.1. Optimization problem

When the area and the material constants of the cells are invariant, the objective function for minimizing the total weight is defined as

$$W_1 = \frac{1}{2}\left(\frac{\tilde{h}}{\tilde{h}_0}\right)^2 \equiv \frac{1}{2}h^2 \tag{9}$$

where h is the thickness of the cell 0 divided by its initial thickness. Besides, the objective function for obtaining the mean stress distribution is defined as

$$W_2 = \frac{1}{2}\left(\frac{\tilde{\sigma}_0}{\sigma_c} - 1\right)^2 \equiv \frac{1}{2}(\sigma_0 - 1)^2 \tag{10}$$

where $\tilde{\sigma}_0$ and σ_c denote the Mises equivalent stress at the cell 0 and the reference stress, respectively.

The CA-constraint condition is defined as

$$g_i = \frac{\tilde{\sigma}_i}{\tilde{\sigma}_i^0} - 1 \equiv \sigma_i - 1 = 0 \qquad (i = 1, \ldots, 8) \tag{11}$$

where $\tilde{\sigma}_i$ and $\tilde{\sigma}_i^0$ denote the Mises equivalent stress at the neighborhood cell i at the present and the preceding steps, respectively.

3.2.2. Derivation of functional

By introducing the weight parameters α and β and the penalty parameter p, we shall define the penalty function,

$$W = \alpha W_1 + \beta W_2 + \frac{p}{2}\sum_{i=1}^{8} g_i^2 = \frac{\alpha}{2}h^2 + \frac{\beta}{2}(\sigma_0 - 1)^2 + \frac{p}{2}\sum_{i=1}^{8}(\sigma_i - 1)^2, \tag{12}$$

where the parameters α and β are defined as

$$\alpha + \beta = 1, \qquad \beta = \begin{cases} \sigma_0 & (\sigma_0 < 1), \\ 1 & (\sigma_0 \geq 1). \end{cases} \tag{13}$$

Expanding Eq. (12) around h, we have

$$W(h+\delta h) \simeq \frac{\alpha}{2}(h+\delta h)^2 + \frac{\beta}{2}(\sigma_0 + \dot{\sigma}_0 \delta h - 1)^2 + \frac{p}{2}\sum_{i=1}^{8}(\sigma_i + \dot{\sigma}_i \delta h - 1)^2 \tag{14}$$

where $\dot{\sigma}_i \equiv \partial\sigma_i/\partial h$, which is the stress design sensitivity. Stationalizing Eq. (14) with respect to h, we have

$$\frac{\partial W(h+\delta h)}{\partial(\delta h)} = \alpha(h+\delta h) + \beta(\sigma_0 + \dot{\sigma}_0\delta h - 1)\dot{\sigma}_0 + p\sum_{i=1}^{8}(\sigma_i + \dot{\sigma}_i\delta h - 1)\dot{\sigma}_i = 0$$

and then,

$$\delta h = -\frac{\alpha h + \beta(\sigma_0 - 1)\dot{\sigma}_0 + p\sum_{i=1}^{8}(\sigma_i - 1)\dot{\sigma}_i}{\alpha + \beta\dot{\sigma}_0^2 + p\sum_{i=1}^{8}\dot{\sigma}_i^2}\,. \tag{15}$$

3.2.3. Derivation of local rule

Equation (15) includes the stress design sensitivity $\dot{\sigma}_i$, which is the first derivative of the equivalent stress with respect to the design variable. We shall introduce here the approximate calculation scheme of the sensitivity.

Assuming that the virtual work theory is held individually for each cell, we have

$$\int_{\Omega_e} \delta\boldsymbol{\varepsilon}^T\boldsymbol{\sigma}\,\mathrm{d}\Omega = \int_{\Gamma_{et}} \delta\mathbf{u}^T\bar{\mathbf{t}}\,\mathrm{d}\Gamma \tag{16}$$

where Ω_e and Γ_e denote the object domain occupied with the element e and its boundary, respectively. Approximating the function distributions on the element with the interpolating function with nodal values, we have

$$h\mathbf{K}'_e\mathbf{U} = \mathbf{f}.$$

Since the matrix $\mathbf{K}'_e$ is independent of the design variable h, direct differentiating the above equation with respect to the design variable h leads to

$$\mathbf{K}'_e\mathbf{U}_e + h\mathbf{K}'_e\dot{\mathbf{U}}_e = \dot{\mathbf{f}} = \mathbf{0}.$$

Finally, we have the displacement sensitivity

$$\dot{\mathbf{U}}_e = -\frac{1}{h}(\mathbf{K}'_e)^{-1}\mathbf{K}'_e\mathbf{U}_e \equiv -\frac{1}{h}\mathbf{U}_e\,. \tag{17}$$

The stress design sensitivity $\dot{\sigma}_i$ is derived from the direct differentiation of Eq. (5) with respect to the design variable h,

$$\dot{\boldsymbol{\sigma}}_e = \mathbf{DB}\dot{\mathbf{U}}_e = -\frac{1}{h}\mathbf{DBU}_e = -\frac{1}{h}\boldsymbol{\sigma}_e\,. \tag{18}$$

Finally, $\dot{\sigma}_i$ in Eq. (14) is given as

$$\dot{\sigma}_i = \frac{\sigma_i}{h}. \tag{19}$$

Substituting Eq. (19) into Eq. (14), we have the local rule,

$$\delta h = \frac{-\alpha h^2 + \beta(\sigma_0 - 1)\sigma_0 + p\sum_{i=1}^{8}(\sigma_i - 1)\sigma_i}{\alpha h^2 + \beta\sigma_0^2 + p\sum_{i=1}^{8}\sigma_i^2}\cdot h. \tag{20}$$

3.3. Rule 2

The design objective, in this case, is to minimize the total weight of the structure. In addition to the CA-constraint condition, it is considered as the constraint conditions, that the Mises equivalent stress at each cell is equal to the reference stress.

3.3.1. Optimization problem

The objective function and the CA-constraint condition are expressed as Eqs. (9) and (11), respectively. Besides, the stress constraint condition is given as

$$g_0 = \frac{\tilde{\sigma}_0}{\sigma_c} - 1 = \sigma_0 - 1 = 0 \tag{21}$$

where $\tilde{\sigma}_0$ and σ_c denote the equivalent stress at the cell and the reference stress of the material, respectively.

3.3.2. Local rule

By introducing the penalty parameter p, the following penalty function can be derived from Eqs. (9), (11) and (21)

$$W = W_1 + \frac{p}{2}\left(g_0^2 + \sum_{i=1}^{8} g_i^2\right) = \frac{1}{2}h^2 + \frac{p}{2}\sum_{i=0}^{8}(\sigma_i - 1)^2 \tag{22}$$

Stationalizing Eq. (22) with respect to h, we have

$$\frac{\partial W}{\partial h} = (h + \delta h) + p\sum_{i=0}^{8}(\sigma_i + \dot{\sigma}_i\delta h - 1)\dot{\sigma}_i = 0 \tag{23}$$

and then,

$$\delta h = -\frac{h + p\sum_{i=0}^{8}(\sigma_i - 1)\dot{\sigma}_i}{1 + p\sum_{i=0}^{8}\dot{\sigma}_i^2}. \tag{24}$$

Substituting Eq. (19) to the above equation, we have the local rule,

$$\delta h = \frac{-h^2 + p\sum_{i=0}^{8}(\sigma_i - 1)\sigma_i}{h^2 + p\sum_{i=1}^{8}\sigma_i^2} \cdot h. \tag{25}$$

3.4. Rule 3

In this case, the design objective is to obtain mean stress distribution on the whole structure and then, only the CA-constraint condition is considered as the constraint condition.

3.4.1. Optimization problem

The objective function and the constraint condition are defined as Eqs. (10) and (11), respectively.

3.4.2. Local rule

By introducing the penalty parameter p, the penalty function is defined from Eqs. (10) and (11) as

$$W = W_2 + p\sum_{i=1}^{8} g_i^2 = \frac{1}{2}(\sigma_0 - 1)^2 + \frac{p}{2}\sum_{i=1}^{8}(\sigma_i - 1)^2. \tag{26}$$

Expanding Eq. (26) around h and stationalizing it, we have

$$\delta h = -\frac{(\sigma_0 - 1)\dot{\sigma}_0 + p\sum_{i=1}^{8}(\sigma_i - 1)\dot{\sigma}_i}{\dot{\sigma}_0^2 + p\sum_{i=1}^{8}\dot{\sigma}_i^2}. \tag{27}$$

Substituting Eq. (19) into the above equation, we have the local rule,

$$\delta h = \frac{(\sigma_0 - 1)\sigma_0 + p\sum_{i=0}^{8}(\sigma_i - 1)\sigma_i}{\sigma_0^2 + p\sum_{i=1}^{8}\sigma_i^2} \cdot h. \tag{28}$$

3.5. Convergence criterion

In the rule 2, the convergence criterion is defined so that the variation of the objective function is smaller than the reference value e,

$$|A^k - A^{k-1}| < e, \tag{29}$$

where A^k denotes the total weight of the structure at k-th step.

In the same manner, the convergence criterion for the rule 3 is defined as follows,

$$|(\sigma)_i - \sigma_c| < e, \tag{30}$$

where $(\sigma)_i$ denotes the equivalent stress at an arbitrary cell.

Finally, the convergence criterion for the rule 1 is defined so that Equations (29) and (30) are satisfied simultaneously.

3.6. Optimization algorithm

The algorithm of the present method is as follows:

1. Input initial data such as size of design domain, boundary condition, number of cells and design conditions.
2. Perform stress analysis with finite element method.
3. Confirm convergence criterion. If the criterion is satisfied, the results are printed out and the process is terminated. If not so, the process goes to the next step.
4. Calculate renewal value of the design variable δh and then, update the design variables by

   $$h^{k+1} = h^k + \delta h.$$
5. Go to Step 2.

In the numerical examples in the following sections, the convergence criterion is not employed because the main object of the examples is to estimate the convergence property of the rules.

4. Numerical example

4.1. Object under consideration

In order to compare the properties of three rules, they are applied to the numerical example shown in Fig. 2. A square domain is taken as an initial design domain. Four corners are fixed and the load P is applied at the center of the domain. The design parameters are specified as shown in Table 1. In the table, σ_0 means the initial maximum stress.

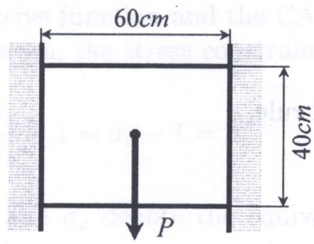

Fig. 2. Object under consideration

Table 1. Design parameters

Number of cells	60×40
Penalty parameter	$p = 10$
Young's modulus	$E = 3.0 \times 10^8$ [Pa]
Poisson's ratio	$\nu = 0.3$
Initial thickness	$h_0 = 10^{-2}$ [m]
Load	$P = 10^3$ [N]
Reference stress	$\sigma_c = 0.8 \times \sigma_0$

4.2. Comparison of convergence properties

Figure 3 shows the results by the rule 1. The total weight of the structure W decreases with the increase of the iteration and finally approaches to about 10% of the initial weight W_0. The maximum stress $\sigma_{\max}$ decreases with the increase of the iteration and approaches to the reference stress $\sigma_c = 0.8 \times \sigma_0$. The mean stress σ_m increases gradually and approaches to the reference stress σ_c.

Figure 4 shows the results by the rule 2. The total weight of the structure W decreases more rapidly than the rule 1 and almost approaches to about 10% of the initial weight at 300-th iteration. Besides, the maximum stress $\sigma_{\max}$ also decreases rapidly and approaches to $0.9 \times \sigma_0$ which is larger than the reference stress $\sigma_c = 0.8 \times \sigma_0$. The maximum stress $\sigma_{\max}$ increases at 2200-th iteration because the stress only at the unique cell increases suddenly. The mean stress σ_m increases gradually and approaches to the reference stress. We notice that the convergence speed of the rule 2 is much

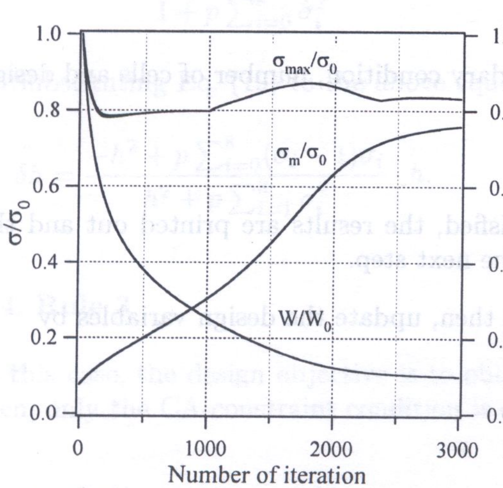

Fig. 3. Convergence histories (rule 1)

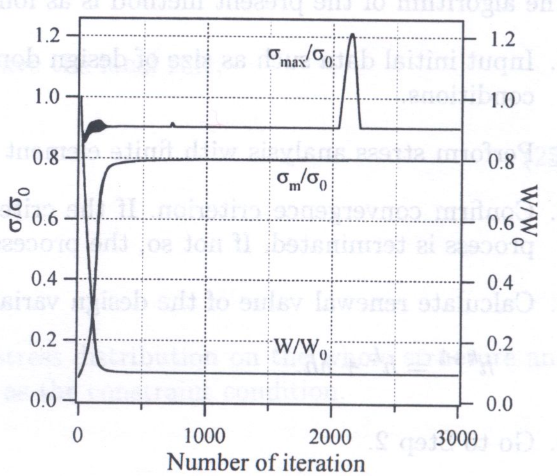

Fig. 4. Convergence histories (rule 2)

faster than the rule 1 and that while the mean stress approaches to the reference stress, the maximum stress dose not approach to the reference stress.

Figure 5 shows the results by the rule 3. The convergence curves of the maximum and the mean stresses are similar to them by the rule 1. Their convergence speed is, however, slower than the rule 1. Although the objective function for minimizing the weight is not considered, the total weight decreases with the increase of the iteration and approaches to about 12% of the initial weight.

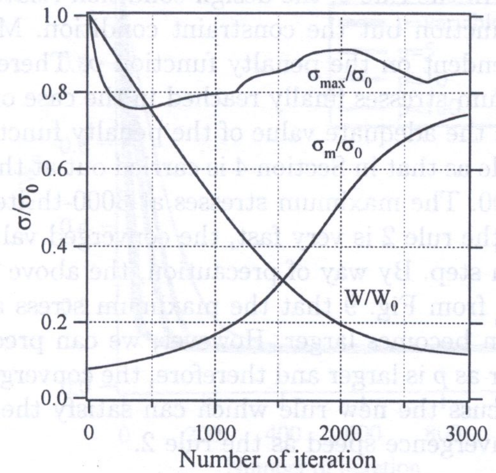

Fig. 5. Convergence histories (rule 3)

4.3. Comparison of final profiles

The distributions of the cell thicknesses at the final profiles are shown in Figs. 6, 7 and 8, respectively. Darker cells mean thicker cells and white cells void. Final profiles are similar to X-shaped truss structures. While thin cells are distributed widely in the final profiles by the rules 1 and 3, the relatively thick cells are placed closely in the final profiles by the rule 2.

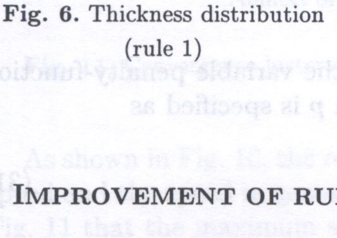

Fig. 6. Thickness distribution (rule 1)

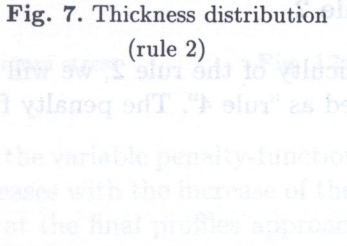

Fig. 7. Thickness distribution (rule 2)

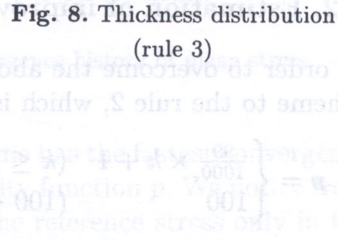

Fig. 8. Thickness distribution (rule 3)

5. IMPROVEMENT OF RULE 2

5.1. Detailed estimation of rules

As shown in the previous section, while the rules 1 and 3 have the similar convergence properties, the convergence speed of the rule 2 is much faster than the other rules.

From the convergence properties of the total weights of the structures, we notice that the final structure in the rule 3 is much heavier than the others. This is because, in the rule 3, the minimization of the total weight is not considered as the objective function.

From the convergence properties of the stress distributions, we notice that while the mean stresses finally approach to the reference stress σ_c in all rules, the maximum stresses approach to σ_c only in the rules 1 and 3. As the reason why, in the rule 2, the maximum stress can not approach to the reference stress, we can point out that reduction of the maximum stress is not considered into the objective function in the rule 2. In the rule 2, the design condition related to the stress distribution is taken as not the objective function but the constraint condition. Moreover, the satisfaction of the constraint condition is dependent on the penalty function p. Therefore, we should discuss the relationship between the maximum stresses finally reached in the case of the rule 2 and the penalty function p in order to determine the adequate value of the penalty function p. For this purpose, the optimization of the same example as that in Section 4 is carried out at the different values of penalty function; $p = 5,\ 10, 100$ and 300. The maximum stresses at 3000-th iteration are shown in Fig. 9. Since the convergence speed of the rule 2 is very fast, the converged values of the maximums stress can be obtained at less iteration step. By way of precaution, the above calculations are carried out by 3000-th iteration. We notice from Fig. 9 that the maximum stress approaches to the reference stress σ_c as the penalty function becomes larger. However, we can predict from Eq. (25) that the update value δh becomes smaller as p is larger and therefore, the convergence speed may be reduced. In the next section, we will discuss the new rule which can satisfy the stress constraint condition and moreover, has the same convergence speed as the rule 2.

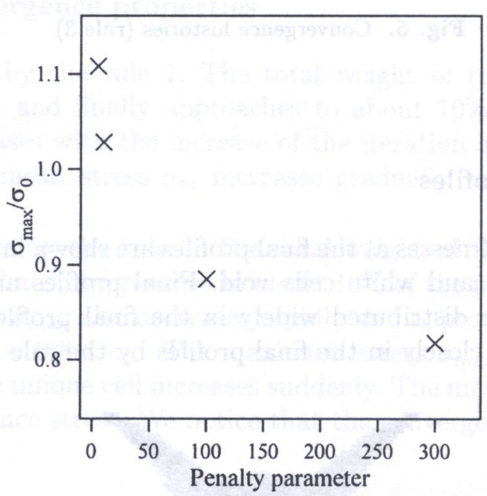

Fig. 9. Maximum stress vs. penalty parameter

5.2. Estimation of improved rule 2

In order to overcome the above difficulty of the rule 2, we will apply the variable penalty-function scheme to the rule 2, which is named as "rule 4". The penalty function p is specified as

$$p = \begin{cases} \frac{99}{1000} \times k + 1 & (k \leq 100), \\ 100 & (100 < k). \end{cases} \tag{31}$$

The value of the function is specified as one at the initial step and then, increases gradually with the number of the iteration.

The rule 4 is applied to the numerical example shown in Fig. 2 with the design condition shown in Table 1. The results by the rule 4 are compared with them in the cases of the unchanged values of the penalty functions. Figures 10, 11 and 12 show the convergence histories of the total weight of the structure and the maximum and the mean stresses, respectively. The label "p=variable" denotes the result in the case of the variable penalty-function scheme. Besides, the labels "$p = 5$", "$p = 10$" and "$p = 100$" mean them in the cases of the unchanged penalty-function schemes of 5, 10 and 100, respectively.

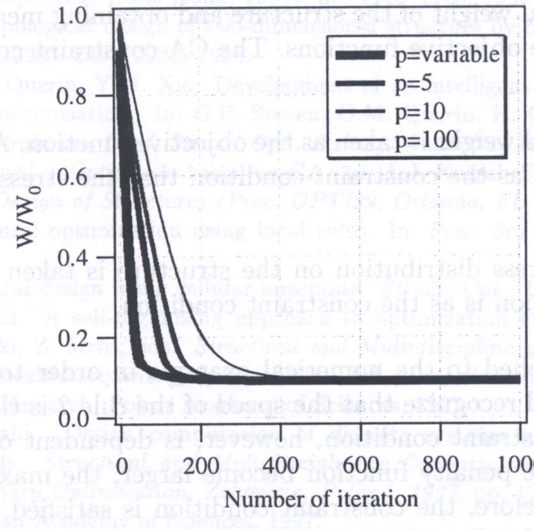

Fig. 10. Convergence history of total weight of structure

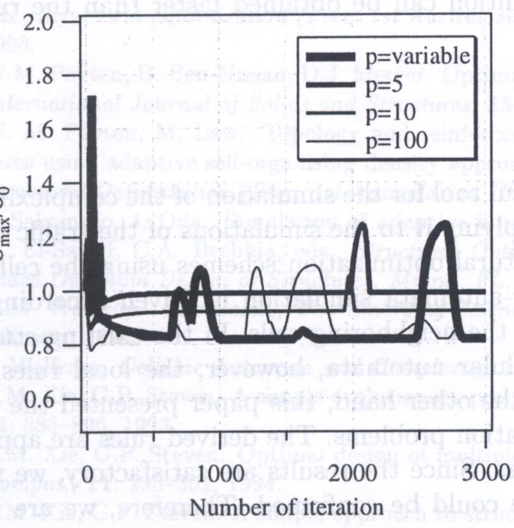

Fig. 11. Convergence history of maximum stress

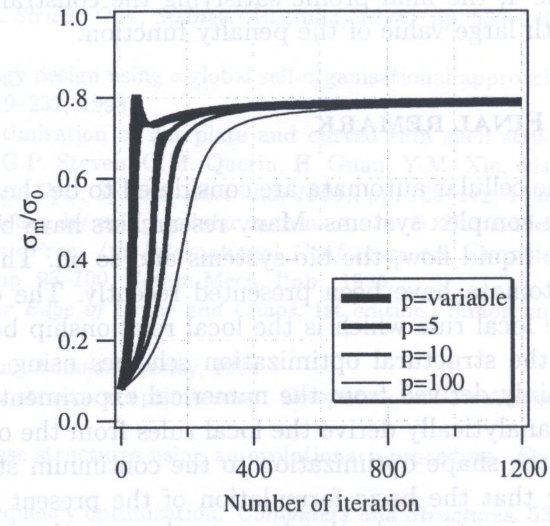

Fig. 12. Convergence history of mean stress

As shown in Fig. 10, the result in the variable penalty-function scheme has the fastest convergence speed and the speed in general decreases with the increase of the penalty function p. We notice from Fig. 11 that the maximum stresses at the final profiles approach to the reference stress only in the cases of $p = 100$ and the variable penalty-function scheme. As shown in Fig. 12, the converge speed of the mean stress is the fastest in the variable penalty-function scheme. Finally, we can say that by using the rule 4, the final profile with the uniform stress distribution can be obtained without the lose of the convergence speed.

6. Conclusions

This paper describes the application of the cellular automata to the shape optimization of the two-dimensional structures. The cellular automata simulation is performed according to the local rule. In this study, the local rule is derived analytically from the optimization problem. Firstly, the different rules are derived from three optimization problems:

Rule 1: Minimizing the total weight of the structure and obtaining mean stress distribution on the structure are taken as the objective functions. The CA-constraint condition is as the constraint condition.

Rule 2: Minimizing the total weight is taken as the objective function. As well as the CA-constraint condition, it is considered as the constraint condition that the stress at each cell is equal to the reference stress.

Rule 3: Obtaining mean stress distribution on the structure is taken as the objective functions. The CA-constraint condition is as the constraint condition.

The derived rules are applied to the numerical example in order to confirm their convergence speed. As the result, we could recognize that the speed of the rule 2 is the fastest among them. The satisfaction of the stress constraint condition, however, is dependent on the value of the penalty function in the rule 2. As the penalty function become larger, the maximum stress approaches to the reference stress and therefore, the constraint condition is satisfied. However, it was predicted that the increase of the penalty function causes the decrease of the convergence speed. Therefore, in order to overcome this difficulty, we finally presented the rule 4 which is composed of the rule 2 and the variable penalty-function scheme. In this rule, the penalty function is specified as one at the initial step and then, increases gradually with the increase of the iteration step. By using the rule 4, the final profile satisfying the constraint condition can be obtained faster than the rule 2 with large value of the penalty function.

7. Final Remark

The cellular automata are considered to be the powerful tool for the simulation of the complexity or the complex systems. Many researchers have been applying it to the simulations of the traffic flow, the liquid flow, the bio-systems and so on. The structural optimization schemes using the cellular automata have been presented recently. The cellular-automata simulation is driven according to the local rule which is the local relationship between the neighboring cells. In the existing studies of the structural optimization schemes using the cellular automata, however, the local rules are mainly derived from the numerical experiments. On the other hand, this paper presented the way to analytically derive the local rules from the optimization problems. The derived rules are applied to the shape optimization to the continuum structures. Since the results are satisfactory, we may say that the basic formulation of the present scheme could be confirmed. Therefore, we are now planning to apply the present scheme to large-scale structures and extend the formulation of the present scheme to the other optimization problems.

References

[1] K.-J. Bathe. *Finite Element Procedures in Engineering Analysis.* Prentice-Hall, 1982.

[2] E.R. BerleKamp, J.H. Conway, R.K. Guy. *Winning Ways for Your Mathematical Plays*, 1st edition. Academic Press Ltd., 1982.

[3] M. Garzon. *Models of Massive Parallelism*, 1st edition. Springer-Verlag, 1995.

[4] R. Gaylord, K. Nishidate. *Modeling Nature: Cellular Automata Simulations with Mathematica*, 1st edition. Springer-Verlag, 1996.

[5] N. Inou. Optimal design methods based on biological information systems (in Japanese). *Journal of Japan Society for Technology of Plasticity*, **35**(4): 316, 1994.
[6] N. Inou, N. Shimotai, T. Uesugi. A cellular automaton generating topological structures. In: A. McDonach, P.T. Gardiner, R.S. McEwen, B. Culshaw, eds., *Proceedings of Second European Conference on Smart Structures and Materials*, 2361, 1994.
[7] N. Inou, T. Uesugi, A. Iwasaki, S. Ujihashi. Self-organization of mechanical structure by cellular automata. In: P. Tong, T.Y. Zhang, J.K. Kim, eds., *Fracture and Strength of Solids Pt 2; Behavior of Materials and Structures (Proc. 3-rd International Conference, Hong Kong, 1997)*, pp. 1115–1120, 1998.
[8] R. Ishida, A. Shiragami. Topological design of two-dimensional structure by cellular automaton (in Japanese). *Transactions of JSME*, **A64**(628): 2895–2900, 1998.
[9] H. Kim, G.P. Steven, Q.M. Querin, Y.M. Xie. Development of an intelligent cavity creation (ICC) algorithm for evolutionary structural optimisation. In: G.P. Steven, O.M. Querin, H. Guan, Y.M. Xie, eds., *Structural Optimization (Proc. 1st Australasian Conf. Struct. Opt., Sydney, Australia, 1998)*, pp. 241–250, 1998.
[10] E. Kita, T. Toyoda. Structural optimization based on CA. In: A.J. Kassab S. Hernandez, C.A. Brebbia, eds., *Computer Aided Optimum Design of Structures (Proc. OPTI99, Orlando, FL, 1999)*, pp. 185–194, 1999.
[11] E. Kita, T. Toyoda. Structural optimization using local rules. In: *Proc. 3rd WCSMO, NY, 1999*, 30-SMO-3, 1999.
[12] E. Kita, T. Toyoda. Structural design using cellular automata. *Struct. Opt.*, **19**: 64–73, 2000.
[13] S. Kundu, J. Oda, T. Koishi. A self-organizing approach to optimization of structural plates using cellular automata. In: W. Gutkowski, Z. Mróz, eds., *Structural and Multidisciplinary Optimization (Proc. 2nd World Congress of Structural and Multidisciplinary Optimization, Zakopane, Poland, 1997*, pp. 173–180. Institute of Fundamental Technological Research, Polish Academy of Sciences, 1997.
[14] S. Kundu, J. Oda, T. Koishi. Design computation of discrete systems using evolutionary learning. In: W. Gutkowski, Z. Mróz, eds., *Structural and Multidisciplinary Optimization (Proc. 2nd World Congress of Structural and Multidisciplinary Optimization, Zakopane, Poland, 1997*, pp. 173–180. Institute of Fundamental Technological Research, Polish Academy of Sciences, 1997.
[15] S. Levy. *Artificial Life, The Quest for a New Creation*, 1st edition. Penguin Books, 1992.
[16] J. von Neumann. *The General and Logical Theory of Automata – Cerebral Mechanisms in Behavior.* John Wiley and Sons, 1951.
[17] J. von Neumann. *Theory of Self-Reproducting Automata.* Illinois Univ. Press, 1966.
[18] W.M. Payten. A fractal interpretation for optimal structures. In: G.P. Steven, O.M. Querin, H.Guan, Y.M. Xie, eds., *Structural Optimization (Proc. 1st Australasian Conf. Struct. Opt., Sydney, Australia, 1998)*, pp. 533–540, 1998.
[19] W.M. Payten, B. Ben-Nissan, D.J. Mercer. Optimal topology design using a global self-organisational approach. *International Journal of Solids and Structures*, **35**(3-4): 219–237, 1998.
[20] W. M. Payten, M. Law. Topology and reinforcement optimisation of flat plate and curved thin shell structures using adaptive self-organising density approach. In: G.P. Steven, O.M. Querin, H. Guan, Y.M. Xie, eds., *Structural Optimization (Proc. 1st Australasian Conf. Struct. Opt., Sydney, Australia, 1998)*, pp. 165–172, 1998.
[21] J. Sakamoto, J. Oda. Simulation of adaptive bone remodeling by using cellular automata. In: S. Hernandez, M. El-Sayed, C.A. Brebbia, eds., *Structural Optimization (Proc. 4th International Conference on Computer Aided Optimum Design of Structures, Miami, FL, 1995)*, pp. 93–100. Comp. Mech. Pub., 1995.
[22] M.M. Waldrop. *Complexity, The Emerging Sciences at the Edge of Order and Chaos*, 1st edition. Simon and Schuster, 1992.
[23] S. Wolfram. *Cellular Automata and Complexity*, 1st edition. Addison-Wesley, 1994.
[24] Y.M. Xie, G.P. Steven. A simple evolutionary procedure for structural optimization. *Computers and Structures*, **49**: 885–896, 1993.
[25] Y.M. Xie, G.P. Steven. Optimal design of multiple load case structures using an evolutionary procedure. *Eng. Comput.*, **11**: 295–302, 1994.
[26] Y.M. Xie, G.P. Steven. A simple approach to structural frequency optimization. *Computers and Structures*, **53**: 1487–1491, 1994.
[27] Y.M. Xie, G.P. Steven. Evolutionary structural optimization for dynamic problems. *Computers and Structures*, **58**(6): 1067–1073, 1996.
[28] X.Y. Yang, Y.M. Xie, G.P. Steven, Q.M. Querin. Bi-directional evolutionary method for frequency optimization. In: G.P. Steven, O.M. Querin, H. Guan, Y.M. Xie, eds., *Structural Optimization (Proc. 1st Australasian Conf. Struct. Opt., Sydney, Australia, 1998)*, pp. 231–237, 1998.
[29] C. Zhao, G.P. Steven, Y.M. Xie. Effect of initial nondesign domain on optimal topologies of structures during natural frequency optimization. *Computers and Structures*, **62**(1): 119–131, 1997.
[30] C. Zhao, G.P. Steven, Y.M. Xie. A generalized evolutionary method for natural frequency optimization of membrane vibration probvlems in finite element analysis. *Computers and Structures*, **66**(2-3): 353–364, 1998.
[31] O.C. Zienkiewicz, R.L. Taylor. *The Finite Element Method*, 4th edition. McGraw-Hill Ltd., 1991.